Markov chain Monte Carlo methods considering the inversion on 1D viscoelastic modeling

Juarez S. Azevedo (Federal University of Bahia, Brazil), Marcio R. Borges (National Laboratory of Scientific Computing, Brazil), and Lucas F. Palma (Federal University of Bahia, Brazil)

Resumo

Markov chain Monte Carlo methods (McMC) have become popular with solving inverse problems in order to derive estimates of original parameters. This methods are characterized by incorporates prior knowledge about the unknown parameters as well as informations about the observations. In this sense, we numerically study the Random Walk (RW) and Differential Evolution (DE) variations of Metropolis algorithm in the context of seismic modeling considering the viscoelastic wave equation. The algorithm is tested for the data from 1987 Superstition Hills earthquake recorded at the Wildlife Site. The results show the effectiveness and accuracy of the algorithms with emphasis to DE-McMC which reached convergence earlier compared to RW.

Introduction

The purpose of this paper is to describe a methodology to compute the probability of the onset of soil properties at a given depth. The 1D viscoelastic wave equation based a smooth hysteretic model is used to characterize the behavior of the soil deposit under random seismic loading (shear modulus reduction and damping ratio) within a Bayesian framework. The Metropolis algorithm and its variants have been widely used in the Bayesian analysis of stochastic inverse problems. Due to the complexity of the modeled systems, the analytical solution for the posterior distribution function may not exist. This leads to the use of numerical methods, such as Markov chain Monte Carlo techniques (McMC), to obtain approximate solutions for the posterior distribution function. The Bayesian framework allows quantifying the added value of information from several sources, while McMC methods allows sampling from the posterior distribution in a computational framework. In this paper, a Random Walk Metropolis (RW) (Sherlock et al., 2010) and a Differential Evaluation Markov Chain Monte Carlo (DE) method (Price et al., 2006) are used to approximate the posterior function and update model.

In the classic version of RW algorithm the new proposal is drawn from a perturbation of the current point of the chain (more details will furnished at section). Often, the *a priori* knowledge about the target distribution is quite limited and the selection and tuning of the proposal distribution may be the bottleneck of the MCMC methods, since they can be inefficient. To overcome this obstacle, a Markov chain Monte Carlo version of the genetic algorithm differential evolution was proposed by Ter Braak (2005), in which multiple chains are run in parallel, to solve the problem of choosing an appropriate scale and orientation for the jumping distribution. The DE jumps are a fixed multiple of the differences of two current random parameter vectors of the chains (population). Recently, Gao et al. (2016) propose a new global optimization algorithm by incorporating a new multimutation scheme into a differential evolution algorithm in seismic inversion problems. Yu et al. (2014) applied the DE for earthquake dislocation source model from the observed crustal deformation field that is a nonlinear multimodal problem. Vrugt (2016) proposed an enhanced version of DE, entitled Differential Evolution Adaptive Metropolis algorithm (DREAM), with self-adaptive randomised subspace sampling.

In practice the DE algorithm estimate the parameters of the geophysical model from a Bayesian structure. This estimate depends on *a priori* information obtained from data and physics of the problem to then estimate a posteriori probability in the model space, which will be the solution to the inverse problem. An important detail is that the DE algorithm do not require knowledge of the posterior probability form, which can be very complicated. Some other advantages can be publicized by this global methods. First, DE is simple to implement and adapt to the inverse problem and this just involves selection for direct modeling. A priori constraints usually define the region of model space to be searched and are explicitly imposed during model selection. Second, the resulting uncertainties may be desirable for the model and summarize the range of models that fit the data and that can be incorporated into the survey. Lastly, the model can be oversized, which is desirable to establish limits that affect the range of such models.

The DE algorithm comes from a new class of global optimization methods that can be used to explore measure motions at the ground surface and within the soil profile. However, this issue of the soil dynamic properties was not properly explored by DE algorithm. We focus in the application of DE to estimate the shear velocity structure from $1D$ viscoelastic shear-wave propagation with a viscous damping model in order to obtain shear displacement on the surface, density, shear modulus and the viscous damping coefficient. Once the inversion is performed, we will compare the results with traditional RW and clearly identify the advantages of this technique for model problem. Random method is applied here using

case histories Wildlife Site, California, seismic vertical arrays considering Superstition Hills recordings of 1987 (Youd & Holzer, 1994). These records were of interest due to liquefaction of the leading site possibly high variability from the data and creating a nonlinear soil behavior interpreted from the recordings.

1D viscoelastic wave equation

Following notation from Oliveira et al. (2018), we will consider the following initial boundary-value problem for the horizontal displacement $u :]0,L[\times]0,T] \to I\!R$:

$$\begin{cases} \rho(z)u_{tt}(z,t) = G(z,t)u_{zz}(z,t) + \eta(z,t)u_{tzz}(z,t), & \\ u(z,0) = u_t(z,0) = 0, & z \in [0,L], \\ u_z(0,t) = 0, \quad u(L,t) = d_1(t), & t \in [0,T]. \end{cases} \tag{1}$$

Herein, sub-indices t and z denote partial derivatives with respect to time and depth, respectively. The coefficient ρ represents density, whereas G is shear modulus and η is the viscous damping coefficient. Function $d_1(t)$ is the recorded downhole horizontal displacement at depth L, and $[0,T]$ is the data recording interval.

We consider a shear modulus reduction relationship introduced by Matasovic & Vucetic (1993):

$$G(z,t) = G_0(z)\sqrt{1-P^\star(z,t)}, \tag{2}$$

where G_0 is the initial shear modulus and $P^\star$ is the excess pore-water pressure ratio. Groholski et al. (2014) refer to the factor $\sqrt{1-P^\star(z,t)}$ as the degradation index, which accounts for the reduction of effective stresses and the corresponding degradation of shear modulus due to excess pore-water pressure generation.

On the other hand, we use the damping coefficient proposed by Ishibashi & Zhang (1993) and defined by:

$$\eta(z,t) = D_0(z)\left[0.586\left(\frac{G(z,t)}{G_{max}}\right)^2 - 1.547\left(\frac{G(z,t)}{G_{max}}\right) + 1\right]G(z,t), \tag{3}$$

where $D_0(z)$ is the damping ratio. We assume the medium is composed of N_l horizontal layers of thickness h_l, $l = 1,\ldots,N_l$, and coefficients ρ, G_0, $P^\star$, and D_0 are homogeneous within each layer, i.e.,

$$\begin{cases} \rho(z) &= \rho_l, \\ G_0(z) &= G_{0,l}, \\ D_0(z) &= D_{0,l} \end{cases} \tag{4}$$

in the l-th layer ($1 \le l \le N_l$). Hence, in order to compute the surface displacement $u(0,t)$ from (1), we need the parameters $\{\rho_l, G_{0,l}, D_{0,l}\}$ for $l = 1,\ldots,N_l$ as well as the time histories of excess pore-water pressure ratios $P_l^\star$ ($1 \le l \le N_l$) and the downhole displacement $d_1(t)$. In numerical discretization, we rewrite $P_e^\star$ ($1 \le e \le N_e$) as $P_e^\star(t) = P^\star(z_e,t)$ and we approximate G and η as follows:

$$\begin{aligned} G_e(t) &\approx G_{0,l}\sqrt{1-P_e^\star(t)}, \\ \eta_e(t) &\approx D_{0,l}\left[0.586\left(\frac{G_l(t)}{G_{max}}\right)^2 - 1.547\left(\frac{G_l(t)}{G_{max}}\right) + 1\right]G_e(t). \end{aligned} \tag{5}$$

Inversion Viscoelastic Model

Let us proceed to the selection of input parameters to the viscoelastic model (1). To infer the excess pore-water pressure ratios $P_l^\star(t)$ at each layer, we follow Oliveira et al. (2018).

Material properties $G_{0,l}$, and $D_{0,l}$, are determined by solving an inverse problem. For this purpose, we define the parameter vector

$$m = [G_{0,1},\ldots,G_{0,N_l},D_{0,1},\ldots,D_{0,N_l}]. \tag{6}$$

Let the predicted surface displacement defined by

$$d(m) = [u_h(0,t_1,m),\ldots,u_h(0,t_M,m)]^T, \tag{7}$$

where $M = N_t$ is the number of observations and $u_h(z,t,m)$ is the surface displacement computed with the spectral element method (Oliveira et al., 2018) when the input data is based on m.

We seek the parameter vector m that minimizes the relative misfit between predicted data $d(m) = [d_1(m),\ldots,d_M(m)]^T$ and the vector of observed surface displacements $d^{obs} = [d_0(t_1),\ldots,d_0(t_M)]^T$, i.e., we seek the solution to

$$\min_{m\in I\!R^N} f(m), \quad f(m) = \frac{\sum_{k=1}^M |d_k^{obs} - d_k(m)|^2}{\sum_{k=1}^M |d_k^{obs}|^2}. \tag{8}$$

The minimization of the misfit function (8) is carried out with the Random Walk Metropolis (**Algorithm 1**) and Differential Evolution Markov Chain (**Algorithm 2**).

Overview of Markov Chain Monte Carlo method

Let us denote the corresponding prior information about the shear modulus and damping ratio field by set m in (6). Using the Bayes's theorem we can write the posterior probability in terms of misfit f:

$$\pi(m) = P(m|f) \propto P(f|m)P(m). \tag{9}$$

where $P(f|m)$ is the likelihood function and $P(m)$ represents the prior distribution. The normalizing constant is ignored due to the iterative search in the McMC algorithm.

In our experiments we admit that the likelihood function is a Gaussian distribution defined by

$$P(f|m) \propto \exp\left(-\frac{f(m)}{\sigma_P^2}\right) \tag{10}$$

where the simulated solution is obtained by spectral discretization for each distribution m in the McMC algorithm.

We adopt McMC method employing the most widely used MH algorithm to explore the posterior distribution as target distribution. The MH uses a proposal distribution $q(m^n,m)$, which depends on the current state m^n, to generate a new proposed sample m. Then, the values proposed are accept with probability

$$\nu(m,m^{(n)}) = \min\left\{1, \frac{q(m|m^n)P(m^n|f)}{q(m^n|m)P(m|f)}\right\} \tag{11}$$

If the proposal is not accepted, then the current value of m is retained: $m^{n+1} = m^n$. In our experiments we assume that proposal distribution is a symmetric distribution $q(m|m^n) = q(m^n|m)$, then it follows that

$$\nu(m, m^{(n)}) = \min\left\{1, \frac{P(m^n|f)}{P(m|f)}\right\}. \quad (12)$$

The MH algorithm will be an essential tool for obtaining adaptive algorithms. We now describe the well known RW and DE algorithms that use the MH algorithm as foundation (Sherri et al., 2019; Ter Braak, 2005).

Random Walk Metropolis

Note that this algorithm just need only a proposal distribution, a function to generate uniform random numbers, and a function to calculate the probability density of each proposal. Operationally, RW algorithm may depend on a large number of samples N_s and the acceptance probability (12). In addition, this single chain method does not have an efficient representation in space of multidimensional parameters if several solutions are locally optimal. Based on the above problem, we are now able to further consider N_c independent chains, which form the multiple Markov chains (Zheng et al., 2013). This suggests a study of multiple chains as summarized in the **Algorithm 1**

Differential Evolution McMC

The Differential Evolution McMC (DE) is an algorithm in which multiple chains are evaluated in parallel simultaneously order to improve the accuracy of the updating parameters. This methodology combines the abilities of the genetic algorithms for global optimization (Sherri et al., 2019) with the MH criterion (Chib & Greenberg, 1995). The idea of the DE method for constructing the test parameters is to generate parameter vectors by adding a weighted difference vector between two population members to a third random vector member. If the resulting vector produces an objective function value smaller than a predetermined population member using the Metropolis-Hasting algorithm, the newly generated vector will replace the vector to which it was compared in the next generation, avoiding problems of premature convergence or loss of fitter individuals throughout the mutation process.

According Vrugt (2016), the procedure is divided into the following steps:

(I) Generate an initial random population of feasible solutions to solve the problem in question, whose parameters to be built are within defined conditions;

(II) An parameter is selected or rejected using the MH algorithm;

(III) With some probability, each variable from the previous process is modified if the parameter was accepted or kept preserved the previous one if the parameter was rejected;

Algorithm 1: RW algorithm

Input:
Initialize chain by sampling from *prior*
$m^{(0)} = [G_{0,1}, \ldots, G_{0,N_l}, D_{0,1}, \ldots, D_{0,N_l}]$;
Set the tuning factor $\gamma = 2.38/\sqrt{2d}$ such that d is the dimension of the updating parameters and
$\gamma_1 \sim U(\gamma, 1)$.
for $j = 1 : N_c$ **do**
  for $n \in \{1, \ldots, N_s\}$ **do**
    $G_e(t) \leftarrow G_{0,l}\sqrt{1 - P_e^\star(t)}$;
    $\eta_e(t) \leftarrow D_{0,l}\left[0.586\left(\frac{G_e(t)}{G_{max}}\right)^2 - 1.547\left(\frac{G_e(t)}{G_{max}}\right) + 1\right] G_e(t)$;
    $m^{(n-1,j)} \leftarrow [G_{0,1}, \ldots, G_{0,N_l}, D_{0,1}, \ldots, D_{0,N_l}]$;
    Propose:
    The random value ε with small variance $\varepsilon \sim N(0, \sigma^2)$;
    $m = m^{(n-1,j)} + \varepsilon$;
    Acceptance Probability:

$$\nu(m, m^{(n-1,j)}) = \min\left\{1, \frac{P(m^{(n-1,j)}|f(m))}{P(m|f(m))}\right\};$$

    $u \sim U(0, 1)$;
    if $u > \nu$ **then**
      Accept the proposal: $m^{(n,j)} \leftarrow m$;
    else
      Reject the proposal: $m^{(n,j)} \leftarrow m^{(n-1,j)}$;
    end
  end
end

DE algorithm solves an important practical problem in RW algorithm, namely, that of choosing an appropriate scale and orientation for the jumping distribution. The algorithm is summarized in the **Algorithm 2**.

Applications

We will now describe a synthetic numerical experiment and apply the DE algorithm presented in the previous section to the Superstition Hills earthquake. The parameters that we wish to infer, described in the numerical experiments are

$$m = [G_{0,1}, \ldots, G_{0,N_l}, D_{0,1}, \ldots, D_{0,N_l}]. \quad (13)$$

In the spatial discretization we use the spectral elements of degree $N_p = 4$, and the time discretization step is $\Delta t = 0.005$ s, so that the predicted data $d(m)$ will have 200 samples per second. Following Oliveira et al. (2018), the number of elements of the mesh is given by $N_e = 9$.

In order to infer the excess pore-water pressure ratios $P_l^\star(t)$ at each layer $l = 1, \ldots, N_l$ we follow the same steps as Oliveira et al. (2018), i.e,

$$P_e^\star(t) = w_{1,e}P_i(t) + w_{2,e}P_j(t), \quad (14)$$

where the weights $w_{1,e}$ and $w_{2,e}$ are fixed in the interpolation. In particular, when the l-th layer is shallower

Algorithm 2: DE algorithm

Input:
Initialize chain by sampling from *prior*
$m^{(0)} = [G_{0,1}, \ldots, G_{0,N_l}, D_{0,1}, \ldots, D_{0,N_l}]$;
Set the tuning factor $\gamma = 2.38/\sqrt{2d}$ such that d is the dimension of the updating parameters and
$\gamma_1 \sim U(\gamma, 1)$.
for $j = 1 : N_c$ **do**
  for $n \in \{1, \ldots, N_s\}$ **do**
    $G_e(t) \leftarrow G_{0,l}\sqrt{1 - P_e^\star(t)}$;
    $\eta_e(t) \leftarrow D_{0,l}\left[0.586\left(\frac{G_e(t)}{G_{max}}\right)^2 - 1.547\left(\frac{G_e(t)}{G_{max}}\right) + 1\right] G_e(t)$;
    $m^{(n-1,j)} \leftarrow [G_{0,1}, \ldots, G_{0,N_l}, D_{0,1}, \ldots, D_{0,N_l}]$;
    Propose:
    Two random vectors m^a, m^b, $m^a \neq m^b \neq m^{(n)}$;
    The random value ε with small variance $\varepsilon \sim N(0, \sigma^2)$;
    $m = m^{(n-1,j)} + \gamma_1(m^a - m^b) + \varepsilon$;
    Acceptance Probability:

$$\nu(m, m^{(n-1,j)}) = \min\left\{1, \frac{P(m^{(n-1,j)}|f(m))}{P(m|f(m))}\right\};$$

    $u \sim U(0,1)$;
    if $u > \nu$ **then**
      Accept the proposal: $m^{(n,j)} \leftarrow m$;
    else
      Reject the proposal: $m^{(n,j)} \leftarrow m^{(n-1,j)}$;
    end
  end
end

or deeper than all observation points:

$$P_e^\star(t) = P_i(t), \quad i = 1, 3, 5, \tag{15}$$

where the piezometers P_1, P_3, and P_5, which are located at depths 5.0 m, 6.6 m, and 2.9 m, respectively. We discard piezometer P_2, since P_5 is more reliable (see Holzer & Youd (2007))

Finally, we need to choose the a priori bounds $[m_i^{min}, m_i^{max}]$ in (13) to get a to be physically meaningful. Thus bounds for shear modulus and damping factor are $G_{0,l} \in [0.9G_{0,l}^r, 1.1G_{0,l}^r]$ $(l = 1, \ldots, N_l)$ and $D_{0,l} \in [0, 0.5]$ $(1 \leq l \leq N_l)$, where $G_{0,l}^r$ is reference value from the literature, specified in the numerical experiments. Moreover, all results shown here are obtained with $N_c = 2d$ independent chains, where d is the number of parameters. This number is justified in Ter Braak & Vrugt (2008) considering a better convergence for simple unimodal targets. In the McMC method we set the following values to standard deviation: $\sigma_P = 0.05$ and $\sigma_P = 0.1$, in order to see how increasing variability changes the solution. For the purposes of this article, it was important to have a relatively accurate estimate of the posterior probability, not determined by RW and DE algorithms. In this sense a "burn in" of 100 iterations was allowed for, and a posterior estimate from the last 2,400 iterations, totalizing $N_s = 2,500$ samples for both algorithms.

The experiments have been implemented in Matlab programming language and have been carried out in a notebook with 16Gb RAM and a 2.40GHz Intel© Core i7-4700HQ processor.

M_1 Model: Wildlife Refuge Site with 4 layers

In this example we replicate the data provided in Oliveira et al. (2018) where we consider a model with $N_l = 4$ layers from Bonilla et al. (2005). The parameters that represent the initial guess in the inversion are given in Table 1. The end time and length are T= 96.98 s, L=7.5 m respectively, and take $d_1(t)$ as the 360-degree (north-south) component of the displacement vector recorded at 7.5 m depth. Here we get the following arrangement for the piezometers:

$$\begin{cases} P_e^\star(t) &= P_5(t) \qquad (1 \leq e \leq 2), \\ P_e^\star(t) &= 0.3P_1(t) + 0.7P_5(t) \quad (3 \leq e \leq 5) \\ P_e^\star(t) &= P_3(t) \qquad (6 \leq e \leq 9) \end{cases} . \tag{16}$$

l	1	2	3	4
h_l (m)	1.5	1	4.3	0.7
ρ_l (kg/m^3)	1600	1928	2000	2000
$G_{0,l}^r$ (kPa)	15681.6	18896.3	26912	26912

Tabela 1 – Thickness (h_l), density (ρ_l), and reference initial shear modulus ($G_{0,l}^r$) of the l-th layer for the 1987 Superstition Hills earthquake.

Figure 1 we display the convergence factor $\hat{R}$ as the number of iterations increases. Here, the number N_c of the Markov chains is equal to 16. We can find that the Markov chains reach convergence with the DE algorithm with just over 700 samples getting close to one (Fig. 1a) while the RW algorithm the diagnostic measure $\hat{R} > 1$, points to that convergence has yet to occur for no value of σ_P.

The minimum misfit $f(m)$ in relation to the RW and DE algorithms and the acceptance rate (AR) are described in Table 2. According to this table, the minimum errors are very close in both methods, while AR is higher in the DE .

	DE		RW	
σ_P	$\min_{m \in \mathbb{R}^N} f(m)$	AR (%)	$\min_{m \in \mathbb{R}^N} f(m)$	AR (%)
0.05	0.2235	47.24	0.2320	24.23
0.1	0.2334	64.93	0.2336	54.58

Tabela 2 – Misfit and acceptance rate of the DE and RW algorithms in model with $N_l = 4$ layers considering $\sigma_P = 0.05$ and $\sigma_P = 0.1$.

Figure 2 exhibits a comparison between reference data and the ensemble average of displacements corresponding to the DE and RW algorithms respectively. We can observe

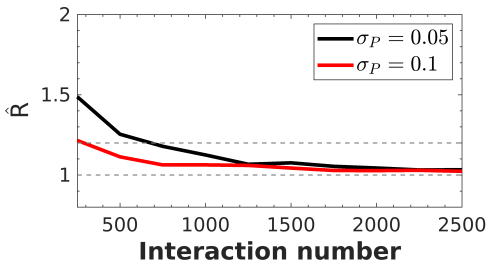

(a)

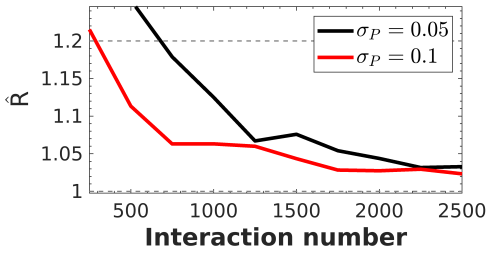

(b)

Figura 1 – Brooks-Gelman convergence factor $\hat{R}$ based on 16 chains. Here, we display the change of the convergence factor $\hat{R}$ of the 16 groups of noise data that are marked with different colors. Horizontal axis represents iteration number and vertical axis represents simulated chains of : (a) DE and (b) RW algorithm.

that both numerical methods have slight differences in relation to the target solution, since both algorithms present very close approximate solutions. In Table 3 we present the values obtained by the inversion of the shear modulus and the damping factor for both algorithms used in the elaboration of these plots. Note that damping ratios are profoundly affected from the third layer, converging to zero in the case of DE. It is probably due to the very pronounced liquefaction phenomena in this layer (Groholski et al., 2014).

Conclusions

The evaluation of convergence factor $\hat{R}$ after each accepted sample illustrated in Figure 1 indicates that the DE has a fast convergence rate and was able to converge after 700 iterations. In this way we can confirm that the DE is characterized by a short period of exploration followed by rapid convergence. The AR value of the updating parameters obtained by the RW algorithm is relatively lower than the DE algorithm. This means that most samples were rejected in the RW resulting in many repeats of the current samples. Despite this, both methods had similar approximations with the reference solution.

$\sigma_P = 0.05$				
	DE		RW	
l	$G_{0,l}$ (kPa)	$D_{0,l}$ (s)	$G_{0,l}$ (kPa)	$D_{0,l}$ (s)
1	16276	0.2030	16308	0.2044
2	19340	0.4353	19400	0.4312
3	26818	0	26921	0.0588
4	25604	0.3254	25658	0.3257
$\sigma_P = 0.1$				
	DE		RW	
l	$G_{0,l}$ (kPa)	$D_{0,l}$ (s)	$G_{0,l}$ (kPa)	$D_{\min,l}$ (s)
1	15820	0.2790	15833	0.2785
2	18975	0.3743	19025	0.3736
3	26804	0	26844	0.0516
4	28305	0.3177	28215	0.3159

Tabela 3 – Mean of estimated parameters for the 1987 Superstition Hills earthquake considering the DE and RW algorithms in the M_1 Model.

Referências

Bonilla, L. F., Archuleta, R. J. & Lavallée, D., 2005. Hysteretic and dilatant behavior of cohesionless soils and their effects on nonlinear site response: Field data observations and modeling, B. Seismol. Soc. Am., vol. 95(6): 2373–2395, doi:10.1785/0120040128.

Chib, S. & Greenberg, E., 1995. Understanding the Metropolis-Hastings algorithm, The american statistician, vol. 49(4): 327–335.

Gao, Z., Pan, Z. & Gao, J., 2016. Multimutation differential evolution algorithm and its application to seismic inversion, IEEE Transactions on Geoscience and Remote Sensing, vol. 54(6): 3626–3636.

Groholski, D. R., Hashash, Y. & Matasovic, N., 2014. Learning of pore pressure response and dynamic soil behavior from downhole array measurements, Soil Dyn. Earthq. Eng., vol. 61: 40–56, doi: 10.1016/j.soildyn.2014.01.018.

Holzer, T. L. & Youd, T. L., 2007. Liquefaction, ground oscillation, and soil deformation at the Wildlife array, California, B. Seismol. Soc. Am., vol. 97(3): 961–976, doi: 10.1785/0120060156.

Ishibashi, I. & Zhang, X., 1993. Unified dynamic shear moduli and damping ratios of sand and clay, Soils Found., vol. 33(1): 182–191, doi:10.3208/sandf1972.33.182.

Matasovic, N. & Vucetic, M., 1993. Cyclic characterization of liquefiable sands, J. Geotech. Eng-ASCE, vol. 119(11): 1805–1822, doi:10.1061/(ASCE)0733-9410(1993)119:11(1805).

Oliveira, S., Azevedo, J. & Porsani, M., 2018. A numerical viscoelastic model of ground response assimilating pore-water pressure measurements., Bollettino di Geofisica Teorica ed Applicata, vol. 59(3).

Price, K., Storn, M. M. & Lampinen, J. A., 2006. Differential evolution: a practical approach to global optimization, Springer Science & Business Media.

Sherlock, C., Fearnhead, P. & Roberts, G. O., 2010. The random walk metropolis: linking theory and practice through a case study, Statistical Science, vol. 25(2): 172–190.

Sherri, M., Boulkaibet, I., Marwala, T. & Friswell, M., 2019. A differential Evolution Markov Chain Monte Carlo Algorithm for Bayesian Model Updating, Special Topics in Structural Dynamics, Volume 5: 115.

Ter Braak, C. J., 2005. Genetic algorithms and Markov chain Monte Carlo: Differential evolution Markov chain makes Bayesian computing easy (revised), Tech. rep., Wageningen UR, Biometris.

Ter Braak, C. J. & Vrugt, J. A., 2008. Differential evolution Markov chain with snooker updater and fewer chains, Statistics and Computing, vol. 18(4): 435–446.

Vrugt, J. A., 2016. Markov chain Monte Carlo simulation using the DREAM software package: Theory, concepts, and MATLAB implementation, Environmental Modelling & Software, vol. 75: 273–316.

Youd, T. L. & Holzer, T., 1994. Piezometer performance at Wildlife liquefaction site, California, J. Geotech. Eng-ASCE, vol. 120(6): 975–995, doi:10.1061/(ASCE)0733-9410(1994)120:6(975).

Yu, Z., Zhaosheng, N. et al., 2014. An improved differential evolution algorithm for nonlinear inversion of earthquake dislocation, Geodesy and Geodynamics, vol. 5(4): 49–56.

Zheng, Z., Wang, H., Gao, S. & Wang, G., 2013. Comparison of multiple random walks strategies for searching networks, Mathematical Problems in Engineering, vol. 2013.

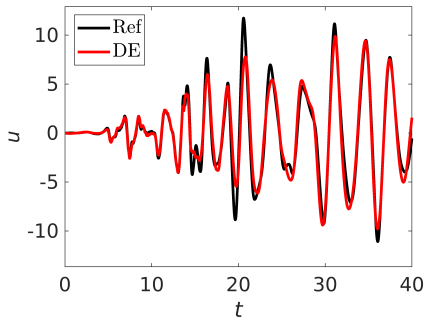

(a) $\sigma_P = 0.05$

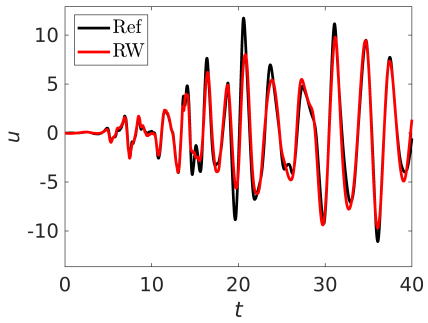

(b) $\sigma_P = 0.05$

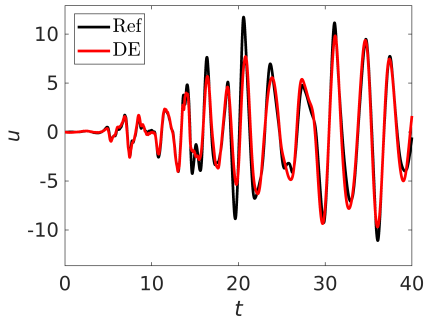

(c) $\sigma_P = 0.1$

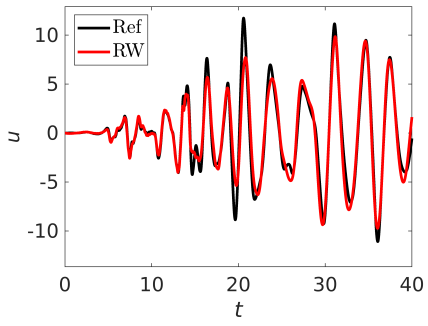

(d) $\sigma_P = 0.1$

Figura 2 – Comparative displacement mean of both the algorithms (DE and RW) for WLA Surface after a burn-in period of 100 samples in M_1 Model considering $\sigma_P = 0.05$ (a)-(b) and $\sigma_P = 0.1$ (c)-(d). Solid lines denote the observed data (black) and numerical solution (red) using DE and RW algorithms.